Proceedings of the 28th IEEE
EMBS Annual International Conference
New York City, USA, Aug 30-Sept 3, 2006

High-Precision Absolute Positioning of Medical Instruments in MRI Systems

Eric Aboussouan, *Student Member IEEE*, and Sylvain Martel*, *Member IEEE*

NanoRobotics Laboratory, Department of Computer Engineering and Institute of Biomedical Engineering,
École Polytechnique de Montréal (EPM), Campus of the Université de Montréal, Montréal (Québec) Canada

*E-mail: sylvain.martel@polymtl.ca URL: www.nano.polymtl.ca

***Abstract*—An absolute positioning technique has been developed for ferromagnetic markers in medical instruments and untethered devices operating in a Magnetic Resonance Imaging (MRI) system. This technique allows high precision 3D readings of the location of the device with respect to the absolute center of the MRI bore. The local magnetic field induced by the device is used as a signature for localization from 3 one-dimensional projections. A convolution between two acquisitions based on opposite read-out gradients is used to obtain the absolute position of the device without any effect from the susceptibility distortion. The validity of the method has been demonstrated and its precision was found sufficient to correctly register the device position with MRI images.**

***Index Terms*—Convolution, absolute positioning, MRI, microdevice, ferromagnetic tracking**

I. INTRODUCTION

Interventional Magnetic Resonance Imaging (IMRI) is a new domain of research on the verge of revolutionizing surgical practices. We are currently designing untethered endovascular microdevices that can be tracked [1-3] and propelled [4] using a conventional Magnetic Resonance Imaging (MRI) system. These microdevices would eventually allow applications such as targeted drug delivery in hard to reach areas of the human vasculature and more specifically, for improving targeting efficacy in chemotherapy and chemo-embolization, to name but only two examples.

Earlier works done by our group have shown that it is possible to obtain a precise 3D position by correlating 3 one-dimensional projections of the magnetic signature of the ferromagnetic device with pre-acquired correlation masks. Unfortunately, this technique only provides readings relative to the initial position of the device and not the absolute positions with respect to the center of the MRI bore. Here, we propose an original method to find the absolute position of the device, thus allowing registration of the device position with pre-acquired images of the patient body and vasculature.

A. Magnetic Signature Projections

When a small microdevice such as a ferromagnetic sphere (but not necessarily spherical) is placed in the magnetic field of an MRI system, it is magnetically saturated and acts like a magnetic dipole. The magnetic gradients generated by this dipole can be used to select a region of the space surrounding the device during a non slice-selective Radio-Frequency (RF) excitation. This excited region will act as a magnetic signature for the tracked device. This signature can be projected on three orthogonal directions of space (x,y,z) using a simple 1D spin-echo or gradient-echo sequence.

B. Geometric Distortions

Because the magnetic field of the dipole remains present during the readout step, the location of the spins is shifted along the read axis as a function of the field strength [5-7]. The perturbed encoded position is given by

$$x' = x + \frac{B'}{G_x} \qquad (1)$$

In (1), x' is the apparent position of the excited spins found at position x, B' is the value of the local dipole magnetic field, and G_x is the readout gradient along the readout axis(x). For projections, this distortion is mostly reflected as an offset location from the apparent position. A loss of symmetry is also observed.

C. Relative Positioning

By correlating the 1D projections obtained at two different times, it is possible to obtain precise information about the relative displacement that occurred. Previous results made with a sphere at a static position give an average error of 0.064 mm between the real displacement and the one measured experimentally. In the dynamic case (i.e. when several acquisitions are repeated rapidly), this value is found to be approximately 1.2 mm [2].

To be able to get an absolute position out of this method, we need to know the exact position of the device during the acquisition of the correlation mask. This could theoretically be done by placement of the ferromagnetic bead in a precise phantom that would be centered as precisely as possible inside the MRI bore. The correlation mask would be acquired, then the phantom removed prior to place the patient inside the bore. This method has several drawbacks. The most important drawback is that the center of the MRI gradients (where the magnetic field is always B_0 when gradients are applied) is known to migrate with time and its

position is difficult to determine precisely. This would add an uncertainty to the position of the bead.

A more suitable approach has been developed, allowing a fast and precise determination of the position of the ferromagnetic entity at any time without requiring any special setup or manipulation while not being affected by the ferromagnetic susceptibility distortion. This auto-calibration method simply involves the convolution of two projections acquired with opposite readout gradients.

II. Theory

A. Absolute Positioning

By taking two readings of a position, one with positive readout gradients and one with negative readout gradients, it is possible to get the absolute position of the device at any time without requiring any specific setup or manipulation. Because the distortion is inversely proportional to the readout gradient, the projection of the magnetic signature will be approximately reversed when the gradient is reversed. Convoluting the projections obtained with opposite gradients will give a maximum at a position related to the center of the device.

To illustrate this method intuitively, let's name $M_+(x)$ a projection mask with a magnetic element arbitrarily placed at x_0 acquired using a positive readout gradient G_R and $M_-(x)$ a mask of the same element, at the same position x_0, taken with the same readout gradient magnitude but pointing in the opposite direction ($-G_R$). Suppose now that $M_+(x)$ is composed of a pattern $A(x-x_0)$. From the above discussion, we can deduce that $M_-(x)$ will be a reflection of the pattern A around x_0, that is $A(x_0-x)$. Convolving M_+ with M^*_-:

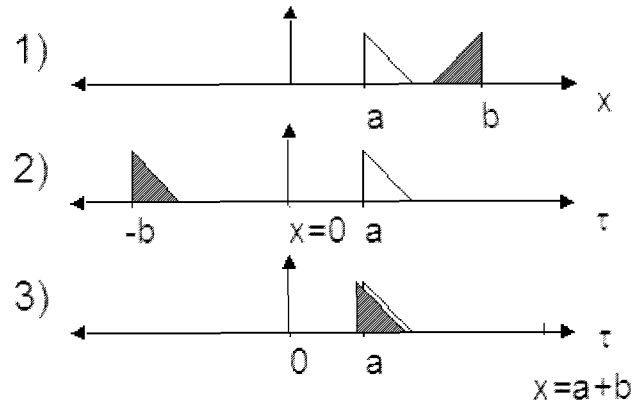

Fig. 1. Intuitive representation of the convolution tracking method for real vectors: 1) $M_+(x)$ and $M_-(x)$, arbitrary real signals displaying symmetry around the position (a+b)/2. 2) $M_-(x-\tau)$ and $M_+(\tau)$ with x=0 3) $M_-(x-\tau)$ and $M_+(\tau)$ with x=a+b.

$$\begin{aligned} C(x) &\equiv M_+(x) \otimes M^*_-(x) \\ &= A(x-x_0) \otimes A^*(x_0-x) \\ &= \int_{-\infty}^{\infty} A(x-x_0-\tau)A^*(x_0-\tau)d\tau \end{aligned} \quad (2)$$

where the superscript * represents the complex conjugate. C(x) will have its global maximum when the two A patterns overlap, that is, for $x=2*x_0$. Knowing x_0, the absolute position of the bead with respect to the center of the MRI bore, it is then possible to use the relative positioning method to get absolute positions by using M_+ as the correlation mask.

B. Practical Implementation

In practice, $M_-(x)$ is already flipped after acquisition because of the negative readout gradient used. The convolution between $M_+(x)$ and $M^*_-(x)$ can thus be implemented as a correlation between $M_+(x)$ and $M_-(-x)$. Intuitively, this is due to the fact that, for two complex vectors M_+ and M_-,

$$\begin{aligned} C(x) = M_+(x) \otimes M^*_-(x) = M_+(x) \bigstar M_-(-x) \\ \text{With } M_+, M_- \in \leq \end{aligned} \quad (3)$$

where $\bigstar$ represents the cross-correlation.

It is important to understand that this is only true because the vector (M) has been flipped as well as the pattern (A) it contains. The vectors M_+ and M_- are also zero-padded to allow the computation in Fourier space without the possible wrap-around due to the implicit redundancy of the Fourier Transform (FT).

III. Method

The experimentation was two-fold. A first test was used to assess the validity of the technique and a second to test its precision. A precisely machined gauge structure was used for the precision test. It was designed to allow a precise displacement of the bead by 15 mm ± 15 μm increments along the x MRI axis. A small socket for the bead was drilled in the setup. The bead could also be removed to allow the imagery of the setup. This experimental setup was calibrated and characterized using a Mitutoyo Legex 9106 Coordinate Measuring Machine (CMM). A maximum assembly imprecision of ± 25 μm was recorded.

The experiments were conducted *in vitro* in a 4 liters phantom filled with water mixed with approximately 20 g/l gelatin, 1.25 g/l nickel sulphate, and 5 g/l NaCl, providing a semi-solid milieu with shortened relaxation times (compared to those of water) to better replicate the relaxation times of the human tissues.

The convolutional tracking was implemented as follows: the projections were acquired using 1D spin-echo-like sequence using 2560μs excitation and rephrasing RF pulses, 1 sec. repetition time, and 1000 Hz frequency offset with a 300 mm field of view. The 1024 points of each vector were written to a file as vectors of 32-bit floating points using a custom image reconstruction program implemented with the Siemens Image Calculation Environment (ICE) architecture.

For each position of the bead, 10 acquisitions were taken with a positive readout gradient and 10 with a negative readout gradient. The projections were analyzed using a custom Matlab™ program. The algorithm described in Sect. II.B was applied for each of these 10 pairs.

A. Validation

The setup was first imaged without the ferromagnetic bead using a gradient echo sequence with pixel sizes 1.3× 0.6×3 mm. A thin wooden stick was inserted in the socket were the bead would later be placed to use it as a fiducial marker in the images. The bead was then inserted in its socket and the global positioning method was applied. The images were analyzed using a custom Matlab™ application. The 512×512 images were displayed and the position of the socket was found semi-automatically. The in-plane position was computed as follows, accordingly to the DICOM standard specification [4]:

$$\begin{bmatrix} P_x \\ P_y \\ P_z \\ 1 \end{bmatrix} = \begin{bmatrix} X_x\Delta i & Y_x\Delta j & 0 & S_x \\ X_y\Delta i & Y_y\Delta j & 0 & S_y \\ X_z\Delta i & Y_z\Delta j & 0 & S_z \\ 0 & 0 & 0 & 1 \end{bmatrix} \begin{bmatrix} i \\ j \\ 0 \\ 1 \end{bmatrix}. \quad (4)$$

where P is the 3D position of the bead, i and j are the pixel coordinates supplied by the user (computed from the upper left corner of the image), X and Y are the direction cosine of the patient image orientation (DICOM attribute #0020,0037), Δi and Δj are the pixel spacing (#0028,0030) and S is the patient image position from the center of the MRI bore (#0020,0032). All distances are in mm.

Each image yielded two usable in-plane coordinates and one coarse through-plane coordinates (corresponding to the center of the slice) that had to be discarded. Five images were used to evaluate the position of the bead socket: two axial images (yielding x and y coordinates), two coronal (x,z) and one sagittal (y,z).

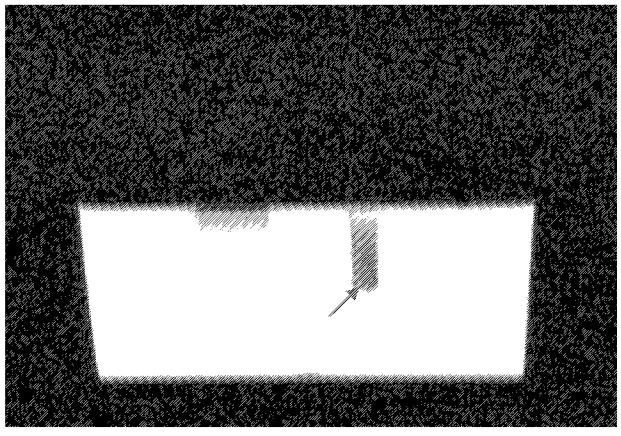

Fig. 2: Example of an MRI image of the setup used to determine the position of the bead socket. The image size is 512×512. The arrow indicates the position of the socket.

B. Precision

The global positioning method was then applied for two different positions 15 mm apart. The positions were then subtracted to compare the observed displacement to the theoretical 15 mm uniaxial increment. The displacement was also compared to the displacement observed using the relative positioning technique described in Sect. I.C.

IV. Results

A. Validation

The results in Table 1 provide the average and standard deviation of the positions estimated by image analysis and convolutional tracking for validation purpose. The average positions estimated with the two methods differ by less then 300 μm on every axis.

The position estimated with the DICOM images, display a standard deviation far greater than the positions estimated with the convolutional tracking method, which leads to think that the latter method is more repeatable. This is due to the lesser resolution of the images and to the difficulty of precisely pinpointing the position of the socket on the images. Note, by comparison, that the resolution of the projections used for the convolutional tracking is given by:

TABLE 1
Validation

	X (mm)	Y(mm)	Z(mm)
	DICOM images :		
Average estimated position:	24.469	41.603	-14.247
Standard deviation :	0.190	0.407	0.399
	Convolutional tracking :		
Average estimated position:	24.316	41.748	-13.975
Standard deviation :	0.000	0.000	0.076
Mean error:	-0.153	0.145	0.273

$$300\text{mm}/1024\text{pixels} = 293\mu\text{m/pixel} \quad (5)$$

and the average error on the position (for a uniform distribution) is given by:

$$\frac{300\text{mm}}{1024\text{pixels}\cdot\sqrt{12}} = 84.6\mu\text{m/pixel} \quad (6)$$

For the DICOM image, the voxel size was 1.3×0.6×3mm and the average error on each axis (using the same calculation) was 375×173×866 μm/pixel.

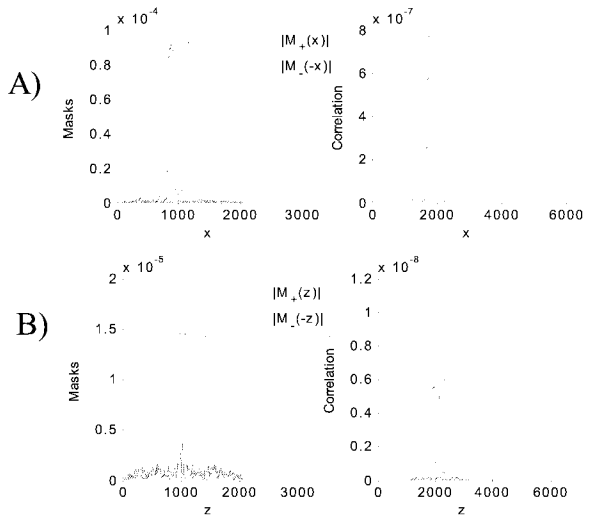

Fig. 3: Examples of projections and their convolution as implemented in Sect. II.B a) Projections on the x axis, b) on the z axis

TABLE 2
Evaluation of the Precision

	X (mm)	Y(mm)	Z(mm)
		Position 1	
Average estimated position:	24.316	41.748	-13.975
Standard deviation :	0.000	0.000	0.076
		Position 2	
Average estimated position:	9.668	41.895	-13.828
Standard deviation :	0.000	0.000	0.076
Distance:	14.648	-0.146	-0.146
Mean error:	0.352	-0.146	-0.146

B. Evaluation of the Precision

The distance between the estimated positions 1 and 2 was evaluated on each axis. The error was first calculated by subtracting the theoretical displacement of 15mm on the x-axis. It was then evaluated using the relative positioning method giving an estimated displacement of 14.648 mm. This leads to think that there was an uncertainty due to the manipulations and that the real precision is actually very close to that of the relative positioning technique (less than 0.1 mm for a static bead). In either case, the precision obtained is sufficient for our applications.

V. Discussion

We proposed a novel technique allowing absolute positioning of a ferromagnetic core in an MRI bore involving the convolution of projections acquired with opposite readout gradients. To speed-up the process, this technique can be used as an auto-calibration method in conjunction with the relative positioning technique already described in [2]. The validity of the technique has been demonstrated and its precision was shown to be sufficient for most tracking applications. This would allow registration of the position of a ferromagnetic marker with pre-acquired images of a patient vasculature.

In the near future, this tracking method will be integrated and tested directly in a Siemens ICE image reconstruction program.

Acknowledgment

This project is supported in part by a Canada Research Chair (CRC) in Micro/Nanosystem Development, Fabrication and Validation, the Canada Foundation for Innovation (CFI), the National Sciences and Engineering Research Council of Canada (NSERC), and the Government of Québec. The authors acknowledge the help from Ouajdi Felfoul, Jean-Baptiste Mathieu as well as the other team members of the MR-Sub project.

References

[1] O. Felfoul, "Technique de positionnement d'objets ferromagnétiques en IRM", Master Thesis, École Polytechnique de Montréal, 2005.

[2] E. Aboussouan, O. Felfoul, J.-B. Mathieu, and S. Martel, "Real-Time projection based technique for tracking ferromagnetic devices", Abstract #3353, *ISMRM Proceedings* , 2006.

[3] J.B. Mathieu, O. Felfoul, S. Martel, G. Beaudoin, (2005), "Magnetic Signature Selective Excitation Tracking", US Provisional Patent Application 60/693,082, June 23, 2005.

[4] J.B. Mathieu, G. Beaudoin, and S. Martel, "Method of propulsion of a ferromagnetic core in the cardiovascular system through magnetic gradients generated by an MRI system" *IEEE Transactions on Biomedical Engineering*, vol. 53, no. 2, pp. 292-299, 2006.

[5] DICOM Standards Committee, "Digital Imaging and Communications in Medicine (DICOM) Part 3: Information Object Definitions", 2004.

[6] J. F. Schenck, "The role of magnetic susceptibility in magnetic resonance imaging : MRI magnetic compatibility of the first and second kinds", *Medical Physics* , vol. 23, pp. 815-850, 1996.

[7] C.J.G. Bakker, R. Bhagwandien, M. A. Moerland, and L. M. P. Ramos, "Simulation of susceptibility artifacts in 2D and 3D Fourier transform spin-echo and gradient-echo magnetic resonance imaging", *Magnetic Resonance Imaging*, vol. 12, no. 5, pp. 767-74, 1994.

[8] A. Ericsson, A. Hemmingsson, B. Jung, and G. O. Sperber, "Calculation of MRI artifacts caused by static field disturbances", *Physics in Medicine and Biology*, vol. 33, no. 10, pp. 1103-12, 1988.